November 28, 2016

QCD Compositeness as Revealed in Exclusive Vector Boson Reactions through Double-Photon Annihilation: $e^+e^- \to \gamma\gamma^* \to \gamma V^0$ and $e^+e^- \to \gamma^*\gamma^* \to V^0V^0$

Stanley J. Brodsky,[1] Richard F. Lebed,[2] and Valery E. Lyubovitskij[3,4,5]

[1]*SLAC National Accelerator Laboratory, Stanford University, Stanford, CA 94309, USA*
[2]*Department of Physics, Arizona State University, Tempe, Arizona 85287-1504, USA*
[3]*Institut für Theoretische Physik, Universität Tübingen, Kepler Center for Astro and Particle Physics, Auf der Morgenstelle 14, D-72076, Tübingen, Germany*
[4]*Department of Physics, Tomsk State University, 634050 Tomsk, Russia*
[5]*Laboratory of Particle Physics, Mathematical Physics Department, Tomsk Polytechnic University, Lenin Avenue 30, 634050 Tomsk, Russia*

We study the exclusive double-photon annihilation processes, $e^+e^- \to \gamma\gamma^* \to \gamma V^0$ and $e^+e^- \to \gamma^*\gamma^* \to V_a^0 V_b^0$, where the V_i^0 is a neutral vector meson produced in the forward kinematical region: $s \gg -t$ and $-t \gg \Lambda^2_{\rm QCD}$. We show how the differential cross sections $\frac{d\sigma}{dt}$, as predicted by QCD, have additional falloff in the momentum transfer squared t due to the QCD compositeness of the hadrons, consistent with the leading-twist fixed-$\theta_{\rm CM}$ scaling laws, both in terms of conventional Feynman diagrams and by using the AdS/QCD holographic model to obtain the results more transparently. However, even though they are exclusive channels and not associated with the conventional electron-positron annihilation process $e^+e^- \to \gamma^* \to q\bar{q}$, these total cross sections $\sigma(e^+e^- \to \gamma V^0)$ and $\sigma(e^+e^- \to V_a^0 V_b^0)$, integrated over the dominant forward- and backward-$\theta_{\rm CM}$ angular domains, scale as $1/s$, and thus contribute to the leading-twist scaling behavior of the ratio $R_{e^+e^-}$. We generalize these results to exclusive double-electroweak vector-boson annihilation processes accompanied by the forward production of hadrons, such as $e^+e^- \to Z^0V^0$ and $e^+e^- \to W^-\rho^+$. These results can also be applied to the exclusive production of exotic hadrons such as tetraquarks, where the cross-section scaling behavior can reveal their multiquark nature.

PACS numbers: 12.38.Aw,12.40.Vv,13.66.Bc,14.40.Be
Keywords: electron-positron annihilation, hadron structure, quantum chromodynamics, vector meson dominance, electroweak bosons, tetraquarks

I. INTRODUCTION

A surprising result, shown by Davier, Peskin, and Snyder (DPS) [1], is that there are exclusive hadronic contributions to the electron-positron annihilation cross section ratio $R_{e^+e^-} = \sigma(e^+e^- \to X)/\sigma(e^+e^- \to \mu^+\mu^-)$ that are scale invariant, but are not associated with the annihilation process $e^+e^- \to \gamma^* \to q\bar{q}$. These exclusive processes are based on double-photon annihilation subprocesses, such as $e^+e^- \to \gamma\gamma^* \to \gamma V^0$ and $e^+e^- \to \gamma^*\gamma^* \to V_a^0 V_b^0$, where the V_i^0 are vector bosons such as the ρ meson. Since the amplitude involves spin-$\frac{1}{2}$ electron exchange in the t and u channels, it behaves as $s^{\frac{1}{2}}$ for $s \gg -t, -u$. The total cross section (which includes a phase-space factor of $1/s^2$), integrated over the dominant forward and backward regions, thus behaves as $1/s$.

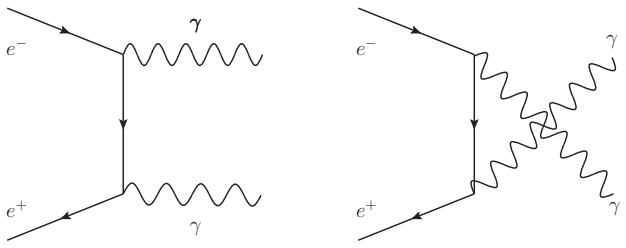

FIG. 1: The double-photon annihilation amplitude in the Born approximation.

In this paper we show how the QCD compositeness of the vector bosons affects the matrix elements and cross sections for these double-photon processes. The effects of compositeness reflect the fact that the coupling of the virtual photon proceeds through the vertex $\gamma^* \to q\bar{q}$. One may study the scaling behavior solely using conventional Feynman diagram techniques, as we describe below and in Sec. II. In order to obtain explicit closed-form results that manifest the correct scaling behavior, we start by employing the light-front quantization of QCD (LF-QCD); in those

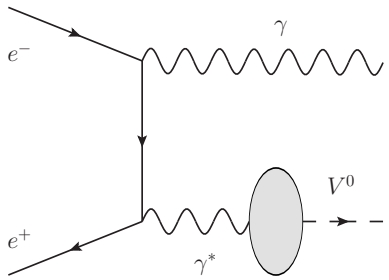

FIG. 2: Exclusive production of a photon and vector boson via double-photon annihilation (the corresponding u-channel diagram is implied). The differential cross section is peaked in the forward and backward directions. Compositeness of the vector boson produces a monopole falloff of the differential cross section $d\sigma/dt$ in $|t|$.

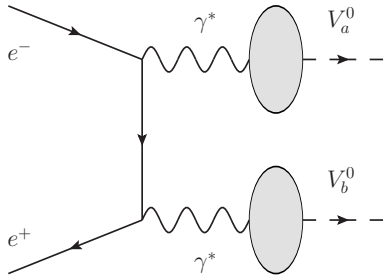

FIG. 3: Exclusive production of two vector bosons via double-virtual photon annihilation (the corresponding u-channel diagram is implied). Compositeness of the vector bosons produces a dipole falloff of the differential cross section $d\sigma/dt$ in $|t|$.

terms, the virtual $q\bar{q}$ then couples to the valence hadronic light-front wave function $\psi_{V^0}(x, \vec{k}_\perp)$. The integration over the light-front momentum fractions $x = k^+/P^+$ and $1-x$, and relative transverse momentum $k_\perp$, of the pair leads to an extra factor of the QCD mass scale $\Lambda_{\rm QCD}$ in the numerator of the amplitude. In order to track both the small- and large-momentum behavior of these processes, we utilize the AdS/QCD (AdS = anti-de Sitter) holographic light-front model [2, 3] which is successful in explaining the main features of meson and baryon spectroscopy, as well as the dynamical properties of hadrons. This nonpertubative approach to hadron physics gives a good overall description of meson and baryon form factors, including consistency with the perturbative QCD (pQCD) power-law scaling of hadronic form factors at large momentum transfer. The AdS/QCD hadronic scale κ can be related to the slope of the Regge trajectories, as well as providing mass relations such as $\kappa = M_\rho/\sqrt{2}$ [2, 3]. We also show that the AdS/QCD prediction for f_ρ, the leptonic decay constant of the ρ meson, is in excellent agreement with measurement.

The double-photon $e^+e^- \to \gamma\gamma$ amplitude illustrated in the first inset of Fig. 1 behaves for large energy as

$$\mathcal{M}(s,t) \propto \alpha_{\rm em}\Big(\frac{s}{-t}\Big)^{\alpha_R} = \alpha_{\rm em}\Big(\frac{s}{-t}\Big)^{1/2}, \tag{1}$$

for $s \gg -t$, corresponding to spin-$\frac{1}{2}$ exchange in the t channel, where the differential cross section is $d\sigma/dt \propto |\mathcal{M}(s,t)|^2/s^2$. The fermion-exchange amplitudes have both t- and u-channel contributions; however, the interference is suppressed in the dominant forward- and backward-peaked domains. As we shall show, and consistent with dimensional analysis, the differential cross section for the production of a single vector meson $\frac{d\sigma}{dt}(e^+e^- \to \gamma V^0)$ via double-photon annihilation (see Fig. 2) must have the extra falloff $G_V^2(t) \sim \kappa^2/|t|$ at large $-t \gg \kappa^2$; *i.e.*,

$$\frac{d\sigma}{dt}(e^+e^- \to \gamma V^0) \sim \frac{\alpha_{\rm em}^3}{s|t|}\frac{\kappa^2}{|t|}. \tag{2}$$

The mass parameter κ is specifically the scale parameter of AdS/QCD approach; however, the power scaling of AdS/QCD and pQCD for $G_V^2(t)$ at large t are the same, consistent with the twist dimension dictated by QCD compositeness. Physically, the extra falloff in $|t|$ results from the phase-space hadronization of the virtual $q\bar{q}$ in the amplitude $e^+e^- \to \gamma q\bar{q} \to \gamma V^0$, which is represented by the transition form factor $G_V(q^2)$. In the case where two vector bosons are produced with opposite transverse momenta (see Fig. 3), the amplitude is suppressed by two form

factors, so the differential cross section at $s \gg -t \gg \kappa^2$ scales as

$$\frac{d\sigma}{dt}(e^+e^- \to \gamma^*\gamma^* \to V_a^0 V_b^0) \sim \frac{\alpha_{\rm em}^4}{s|t|}\frac{\kappa^4}{t^2}\,. \tag{3}$$

The powers of $\alpha_{\rm em}$ correspond to the couplings of the virtual photons to the currents of the annihilating leptons and the vector bosons. In effect, the cross sections are the same as that given by the naive vector-meson dominance (VMD) model [4] but multiplied by the form factors required by QCD compositeness. It is worth noting that such nontrivial form factors also naturally arise in chiral perturbation theory calculations [5, 6], but carry a different scaling, as discussed below.

The scaling results for the exclusive cross sections are consistent with the leading-twist quark fixed-angle counting rules [7–9] : $\frac{d\sigma}{dt}(A+B \to C+D) \propto F(\theta_{\rm CM})/s^{N-2}$, where $N = N_A + N_B + N_C + N_D$ is the total twist or number of elementary constituents. In our case, $N-2=3$ for $e^+e^- \to \gamma V^0$ and $N-2=4$ for $e^+e^- \to V_a^0 V_b^0$, which would give the scaling for non-forward angles (where s, $-t$, $-u$ are all of comparable size). In the present case, the integration over the forward peaks in t and u does not modify the $1/s$ scaling of the total cross section; *e.g.*, $\sigma_{e^+e^-\to\gamma V^0}(s) \propto \alpha_{\rm em}^3/s$, up to logarithms in t (or u), which are cut off by the mass scales in the process: m_e^2 from the propagator between the photons and κ^2 from the dominant part of the hadronization integral.

Although compositeness does not affect the leading $1/s$ scaling of the total cross sections of these reactions, it does strongly modify the t and u dependence of the amplitudes in terms of new types of transition form factors. An analysis such as that given in Ref. [10], based on an effective field theory in which the vector mesons are treated as elementary fields, cannot yield the form factors and counting rules predicted by QCD due to meson compositeness.

In addition, QCD also predicts the $\frac{1}{M_{V_i^0}^2}$ falloff of the amplitudes as the mass of each vector boson is increased; this falloff corresponds to the timelike q^2 of the virtual photon. One thus finds new tests of color confinement and the nonperturbative hadronic wave functions of hadrons. We also show that these results can be extended to electroweak exclusive processes involving electron or neutrino exchange, such as $e^+e^- \to Z^0V^0$, which are accessible at the proposed International Lepton Collider (ILC), and to exotic multi-quark hadrons.

II. COUPLING OF VIRTUAL PHOTONS TO VECTOR BOSONS

In this section we demonstrate how the correct momentum dependence (consistent with QCD compositeness) of the $\gamma^* \to V^0$ transition amplitude can be evaluated in the AdS/QCD approach. The full q^2 dependence of the corresponding transition form factor is model dependent, but at large values of q^2, its scaling must be consistent with pQCD.

First, we point out that the full off-shell $\gamma^*(q) \to V^{0*}(q)$ transition is given by the amplitude $G_V(q^2)(g^{\mu\nu}q^2 - q^\mu q^\nu)/q^2$, where the tensor guarantees gauge invariance, the $1/q^2$ comes from the virtual photon propagator, and the form factor $G_V(q^2)$ has the falloff $1/\sqrt{q^2}$ at large q^2. Therefore, the $\gamma^*(q) \to V^{0*}(q)$ transition scales as $\mathcal{O}(1/\sqrt{q^2})$ at large q^2. This scaling is interesting—it says that the couplings of heavier vector mesons $q^2 = m_V^2$ become increasingly suppressed—but it is not the primary scaling of interest in this paper. In an effective theory that treats the ρ meson as an elementary field, the form factor $G_V(q^2)$ is a constant. In addition, the contributions of the relevant diagrams are different in VMD and pQCD. For example, in the case of the pion electromagnetic form factor, in VMD the contact diagram gives 1 (a constant contribution at large q^2), whereas the vector-meson exchange diagram gives a $(-1 + M_V^2/q^2)$ contribution. Summing these two diagrams, we arrive at a M_V^2/t scaling. In contrast, using pQCD counting rules, the contact diagram turns out to be at leading order $(1/q^2)$, whereas the vector-meson exchange diagram is subleading $[(1/q^2)^{3/2}]$ at large q^2.

The calculation of the transition form factor $G_V(q^2)$ can be performed in soft-wall AdS/QCD [11]. We begin by proposing an effective action describing the coupling of the stress tensors of two vector fields F_{MN} and V_{MN}, which are holographically equivalent to the electromagnetic and neutral vector meson fields, respectively:

$$S = -\frac{1}{2}\int d^4x\, dz\, g_V^{(\kappa)}(z) e^{-\kappa^2 z^2} F_{MN}(x,z) V^{MN}(x,z)\,, \tag{4}$$

where $g_V^{(\kappa)}(z) \equiv \frac{2\kappa}{\sqrt{\pi}}\, g_V z^0$ is the 5-dimensional coupling constant (which, in this special case, is independent of z) and κ is the dilaton parameter. As seen below, g_V arises as the value of $G_V(q^2)$ at $q^2 = 0$.

The matrix element of the $\gamma^*(q) \to V^{0*}(q)$ transition is given by

$$\mathcal{M}_{\rm inv}^{\mu\nu}(q) = -ie\, G_V(q^2)(q^2 g^{\mu\nu} - q^\mu q^\nu)\,, \tag{5}$$

where $G_V(q^2)$ is the transition form factor, which in the Euclidean region is given by

$$G_V(Q^2) = \int_0^\infty dz\, e^{-\kappa^2 z^2} g_V^{(\kappa)}(z) V^2(Q,z)\,, \tag{6}$$

where, in terms of the Kummer (confluent hypergeometric) function U,

$$V(Q,z) = \kappa^2 z^2 \int_0^1 \frac{dx}{(1-x)^2} x^{Q^2/(4\kappa^2)} e^{-\kappa^2 z^2 x/(1-x)} = \Gamma(1+a)\, U(a,0,\kappa^2 z^2) \tag{7}$$

is the bulk-to-boundary propagator for both the F_{MN} and V_{MN} fields [2, 3], and $a = Q^2/(4\kappa^2)$. $V(Q,z)$ obeys the following normalization conditions:

$$V(0,z) = 1\,, \quad V(Q,0) = 1\,, \quad V(Q,\infty) = 0\,. \tag{8}$$

From the first of these conditions and Eq. (6), one easily sees that $G_V(0) = g_V$. As $Q^2 \to \infty$, the vector-field bulk-to-boundary propagator behaves as

$$\begin{aligned} V(Q,z) \;&\to\; \frac{Q^2 z^2}{4} \int_0^\infty \frac{dt}{t^2}\, e^{\kappa^2 z^2 - t - Q^2 z^2/(4t)} \\ &=\; e^{\kappa^2 z^2} Q z\, K_1(Qz)\,, \end{aligned} \tag{9}$$

where $K_1(x)$ is the modified Bessel function of the second kind, which for arbitrary n is given by the integral representation

$$K_n(x) = \frac{x^n}{2^{n+1}} \int_0^\infty \frac{dt}{t^{n+1}}\, e^{-t - x^2/(4t)}\,. \tag{10}$$

One can see that in the limit $\kappa \to 0$, the bulk-to-boundary propagator $V(Q,z)$ in the soft-wall model coincides with the one in the hard-wall model [12]. This expression for $V(Q,z)$ gives the scaling of $G_V(Q^2) \sim 1/\sqrt{Q^2}$ for large Q^2, consistent with quark-counting rules [7–9]:

$$\begin{aligned} G_V(Q^2) \;&=\; \frac{2 g_V}{\sqrt{\pi}}\, \frac{\kappa}{\sqrt{Q^2}} \int_0^\infty dx\, x^2 \Big[K_1(x)\Big]^2 \,+\, \mathcal{O}(1/Q^2) \\ &=\; 1.044\, g_V\, \frac{\kappa}{\sqrt{Q^2}} \,+\, \mathcal{O}(1/Q^2)\,, \end{aligned} \tag{11}$$

since

$$\int_0^\infty dx\, x^2 \Big[K_1(x)\Big]^2 = \frac{3\pi^2}{32} \simeq 0.925\,. \tag{12}$$

Had the coupling $g_V^\kappa(z)$ below Eq. (4) been chosen to scale as z^n, a similar calculation would produce the form-factor scaling $1/(Q^2)^{(n+1)/2}$. Our choice $n = 0$ is the unique one providing a bulk-independent transition between the photon and V mesons, which one expects in AdS/QCD since it mixes with the z-independent kinetic terms $F_{MN}F^{MN}$ and $V_{MN}V^{MN}$.

Note the difference of our approach and the VMD model using an effective elementary field for the vector mesons is that we take into account the Q^2 dependence $G_V(Q^2)$, which leads to an additional suppression due to ρ-meson compositeness; in contrast, in the VMD model, this coupling is just a constant. To model this result, the large-Q^2 dependence of the $G_V(Q^2)$ transition form factor calculated in a soft-wall AdS/QCD model can be approximated by the form

$$\frac{G_V(Q^2)}{G_V(0)} = \frac{1}{1 + \sqrt{Q^2}/\Lambda_V}\,, \tag{13}$$

where $\Lambda_V = 1.044\,\kappa \simeq \kappa$ is the scale parameter. In the numerical evaluation, we use $\kappa \simeq 0.5$ GeV and get $\Lambda_V = 0.522$ GeV. This value follows from the slopes of the hadron Regge trajectories and from the matching of the soft-wall potential with the lattice-QCD heavy-quark potential, leading to $\kappa^2 \simeq \sigma$, where σ is the string tension [13, 14].

For the case of the ρ meson, the value $G_\rho(0) = g_\rho = 0.048$ is fixed from the condition that $G_\rho(Q^2)$ determined from Eqs. (6) and (7) at the vector-meson mass shell $Q^2 = -t = -M_\rho^2$, so that $F_\rho \equiv G_\rho(-M_\rho^2) = 0.202$. F_ρ, in turn, is the so-called leptonic decay constant fixed from the central value of the data on the $\rho^0 \to e^+e^-$ decay width, and is given by the formula [15]:

$$\Gamma(\rho^0 \to e^+e^-) = \frac{4\pi}{3}\alpha_{\rm em}^2 F_\rho^2 M_\rho\,. \tag{14}$$

The form factor $G_V(Q^2)$ very rapidly reaches its asymptotic value. For example, for $\kappa = 0.5$ GeV, the idealized form of Eq. (13) reaches about 80% of its asymptotic value $1.044\,g_V\kappa/\sqrt{Q^2}$ already by $Q^2 = 4$ GeV^2. The approach to the asymptote for the exact result is even faster. In Fig. 4 we plot the result for the exact form factor $\sqrt{Q^2}G_V(Q^2)/G_V(0)$ obtained from Eqs. (6) and (7) and compare it with asymptotic line $1.044\,\kappa$ deduced from Eq. (11).

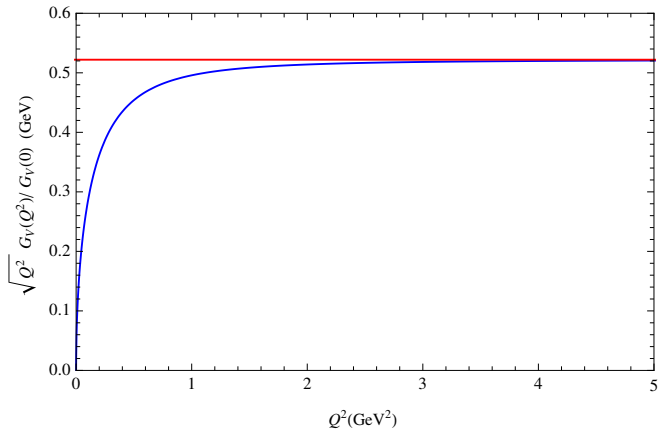

FIG. 4: The form factor $\sqrt{Q^2}G_V(Q^2)/G_V(0)$. The horizontal line 1.044κ corresponds to its asymptotic value at large Q^2.

On the other hand, the value of the coupling F_ρ can be calculated in LF-QCD, using [3]

$$F_\rho = 2\frac{\sqrt{N_c}}{M_\rho}\int_0^1 dx \int \frac{d^2k_\perp}{16\pi^3}\,\psi_L(x,k_\perp)\,, \tag{15}$$

where $\psi_L(x,k_\perp)$ is the longitudinal light-front wave function (LFWF) of the ρ meson, and $N_c = 3$. It is known from the matching of LF-QCD to soft-wall AdS/QCD that [16]

$$\psi_L(x,k_\perp) = \frac{4\pi}{\kappa}\,\frac{\sqrt{\log(1/x)}}{1-x}\,\exp\left[-\frac{k_\perp^2}{2\kappa^2}\,\frac{\log(1/x)}{(1-x)^2}\right]. \tag{16}$$

Straightforward calculation gives

$$F_\rho = \frac{\kappa}{M_\rho}\sqrt{\frac{N_c}{\pi}}\left(1-\frac{1}{\sqrt{2}}\right). \tag{17}$$

Using the value $M_\rho = 755.26$ MeV, one obtains from this process that $F_\rho \simeq 0.185$, which compares well with the experimental value $F_\rho = 0.202$ given above. Note that using the prediction of the AdS/QCD for the ρ meson mass $M_\rho = \kappa\sqrt{2}$ [2, 3] gives startling agreement of the calculated value of F_ρ with data:

$$F_\rho = \sqrt{\frac{N_c}{2\pi}}\left(1-\frac{1}{\sqrt{2}}\right) \simeq 0.202\,. \tag{18}$$

Note that the $\gamma^*(q) \to V^{0*}(q)$ transition itself [without the form factor G_V] has no additional falloff in q^2, because the q^2 from the Lorentz structure of Eq. (5) is compensated by the $1/q^2$ from the virtual photon. This result is

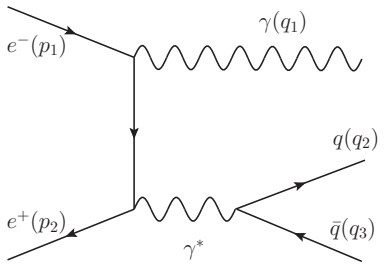

FIG. 5: Diagram contributing to the $e^+e^- \to \gamma\gamma^* \to \gamma q\bar{q}$ annihilation (the corresponding u-channel diagram is implied).

consistent with the VMD model, which is based on the constant behavior of the $\gamma^*(q) \to V(q)$ transition. The main difference from VMD model is that QCD compositeness gives a nontrivial t dependence, as discussed below. In particular, let us evaluate the matrix element for the process $e^+e^- \to \gamma\gamma^* \to \gamma V^0$; it is effectively given by the product of the matrix elements of the perturbative process $e^+e^- \to \gamma\gamma^* \to \gamma q\bar{q}$ and the nonperturbative process $\bar{q}q \to V^0$:

$$\mathcal{M}(e^+e^- \to \gamma V^0) = \mathcal{M}(e^+e^- \to \gamma q\bar{q})\, \mathcal{M}(\bar{q}q \to V^0)\,, \tag{19}$$

where the perturbative matrix element includes the sum of t and u channels (see Fig. 5):

$$\mathcal{M}(e^+e^- \to \gamma q\bar{q}) = e^3 \bar{v}(p_2) \left[\gamma^\nu \frac{1}{\not{k}} \gamma^\mu + \gamma^\mu \frac{1}{\not{\tilde{k}}} \gamma^\nu\right] u(p_1)\, \frac{1}{s_2}\, e_q\, \bar{u}(q_2)\gamma_\nu v(q_3)\, \epsilon^*_\mu(q_1)\,, \tag{20}$$

with e_q being the quark charge, $s + t + u = s_2$, $s_2 = q^2 = (q_2 + q_3)^2$, $k = p_1 - q_1$, $\tilde{k} = q_1 - p_2$. Next, using Eq. (5) and the transversity condition $q \cdot \epsilon^*(q) = 0$ for vector particles V^0, we replace the product of the final-state bilinear and $\mathcal{M}(\bar{q}q \to V^0)$ by

$$e_q\, \bar{u}(q_2)\gamma_\nu v(q_3) \times \mathcal{M}(\bar{q}q \to \tilde{V}^0) \to \tilde{G}_V(s_2; -t)\, s_2\, \epsilon^*_\nu(q)\,, \tag{21}$$

where the coupling function $\tilde{G}_V(s_2; -t)$ describes the $\gamma^* \to q\bar{q} \to \tilde{V}^0$ transition. At this stage, $\tilde{G}_V$ is an inclusive coupling to a neutral vector source $\tilde{V}^0$ at momentum transfer s_2 and does not yet refer to a single vector particle V^0 of a particular mass $\sqrt{s_2}$. If s_2 is not otherwise constrained, one expects it generically to be of order $-t$, as indicated by the second argument of $\tilde{G}_V$. The key point to notice is that the proper amplitude to use for a particular process depends not only upon the momentum transfer s_2 entering from the virtual photon, but it is further constrained by which distinct exclusive final state it becomes; in particular, if we consider it to be the exclusive transition form factor $G_V(s_2)$ referring to a single vector meson V^0. Generically, the $q\bar{q}$ pair in Fig. 5 emerges with a large transverse momentum and creates a number of hadrons through fragmentation; even if s_2 is taken to be as small as M_ρ^2, one can still produce up to 5 pions from the γ^*. For example, in order to produce a single vector meson exclusively, whose constituent quarks are nearly collinear, typically requires the exchange of a hard gluon between the $q\bar{q}$ pair, such that the gluon momentum transfer is of the order of $-t$. Taking into account this physical constraint, which arises due to QCD compositeness of the hadron, is essential for obtaining correct scaling of the form factor G_V for large $-t$; we recognize this fact by henceforth restricting $\tilde{G}_V(s_2; -t) \to G_V(M_V^2; -t) \equiv G_V(-t)$, the transition form factor for a single vector meson V^0 of mass M_V.

Were one to insert a hard gluon line between q_2 and q_3 in Fig. 5 to form a loop, each end of the (initially) hard quarks q_2 and q_3 would provide a spinor normalization factor $\sim |t|^{1/4}$ and each hard quark (gluon) propagator would contribute a factor $\sim 1/|t|^{1/2}$ ($\sim 1/|t|$). The loop integral naively would bring in four powers of momentum, but the leading-order piece gives rise to the divergence of the vertex correction, which is subtracted, and the cubic piece gives an odd function, which vanishes under integration. Thus the loop integral gives a contribution $\sim |t|$, so that one expects $G_V(-t)$ for large $|t|$ to scale as $1/|t|^{1/2}$.

Finally, we obtain

$$\mathcal{M}(e^+e^- \to \gamma V^0) \;=\; e^3\, G_V(-t)\, \bar{v}(p_2) \left[\gamma^\nu \frac{1}{\not{k}} \gamma^\mu + \gamma^\mu \frac{1}{\not{\tilde{k}}} \gamma^\nu\right] u(p_1)\, \epsilon^*_\nu(q)\, \epsilon^*_\mu(q_1)\,. \tag{22}$$

In comparing with Eq. (20) one sees that, as in the VMD model, the denominator of the virtual photon propagator (s_2) is compensated by the factor s_2 coming from the Lorentz structure of the $\bar{q}q \to V^0$ transition. On the other

hand, one sees the important difference from the VMD model: Our coupling $G_V(-t)$ has explicit dependence on t and falls off as $1/|t|^{1/2}$ at large $|t|$.

Our kinematical limit is as follows: We consider the small forward-angle (θ) scattering region to be such that $-t \sim s \cdot \theta^2$, while $s_2 = M_V^2 \ll -t$ satisfies $s + t + u = s_2$. The differential cross section $d\sigma/dt$ for the process $e^+e^- \to \gamma V^0$, where V^0 is any neutral vector-meson state, is calculated according to the formula

$$\frac{d\sigma}{dt} = \frac{1}{64\pi^2 s^2} \sum_{\rm pol} |\mathcal{M}(e^+e^- \to \gamma V^0)|^2 \,. \tag{23}$$

After a straightforward calculation, we obtain

$$\frac{d\sigma}{dt} \;=\; \frac{8\pi\alpha_{\rm em}^3}{s|t|}\, G_V^2(-t) \Big[1 + \frac{t}{s} + \mathcal{O}(1/s^2)\Big] \,. \tag{24}$$

At large $-t$, the differential cross section scales as

$$\frac{d\sigma}{dt} \sim \alpha_{\rm em}^3 \, \frac{\kappa^2}{st^2} \,. \tag{25}$$

For the process $e^+e^- \to V_a^0 V_b^0$, we use the following kinematics:

$$s + t + u = s_{2a} + s_{2b} \,, \tag{26}$$

where $s_{2a} = q_a^2 = M_{V_a}^2$ and $s_{2a} = q_b^2 = M_{V_b}^2$, and $s \gg -t \gg s_{2a}$, s_{2b}. The differential cross section is given by

$$\frac{d\sigma}{dt} \;=\; \frac{1}{64\pi^2 s^2} \sum_{\rm pol} |\mathcal{M}(e^+e^- \to V_a^0 V_b^0)|^2 \,, \tag{27}$$

where

$$\mathcal{M}(e^+e^- \to V_a^0 V_b^0) \;=\; e^4\, G_V^2(-t)\, \bar v(p_2) \Big[\gamma^\nu \frac{1}{\not k} \gamma^\mu + \gamma^\mu \frac{1}{\tilde{\not k}} \gamma^\nu\Big]\, u(p_1)\, \epsilon_\nu^*(q_b)\, \epsilon_\mu^*(q_a) \,. \tag{28}$$

From this amplitude, one can compute:

$$\frac{d\sigma}{dt} \;=\; \frac{32\pi^2\alpha_{\rm em}^4}{s|t|}\, G_V^4(-t) \Big[1 + \frac{t}{s} + \mathcal{O}(1/s^2)\Big] \,. \tag{29}$$

The falloff of $\frac{d\sigma}{dt}$ for double-vector meson production at large t is thus

$$\frac{d\sigma}{dt} \sim \alpha_{\rm em}^4 \, \frac{\kappa^4}{s|t|^3} \,. \tag{30}$$

Our finding is relevant for the process of dilepton production in e^+e^- annihilation, when the neutral vector meson produces the lepton pair. In this case, each vector meson gives a $1/t^2$ falloff in the cross section, due to the falloff of the vector-meson form factor $G_V(-t) \sim 1/|t|^{1/2}$ at large $-t$.

III. ANNIHILATION $e^+e^- \to Z_c^+\pi^-$ AND $e^+e^- \to Z_c^+ Z_c^-$

Using soft-wall AdS/QCD, we can derive the universal formula for the ratio

$$R = \frac{\sigma(e^+ + e^- \to H_{n_1} + H_{n_2})}{\sigma(e^+ + e^- \to \mu^+ + \mu^-)} \,, \tag{31}$$

where n_1 and n_2 are the numbers of partons in each hadron.

According to Ref. [17], the ratio R is given by the square of the $\gamma \to H_{n_1} + H_{n_2}$ transition form factor:

$$R = |F_{H_{n_1} H_{n_2}}(s)|^2 \,. \tag{32}$$

Note that these functions F are the more conventional electromagnetic form factors (coupling two states to a photon), in distinction to the transition form factors G_V (coupling a photon to a single state) discussed in the previous section. In the soft-wall AdS/QCD model, $F_{H_{n_1}H_{n_2}}(Q^2)$ is given by

$$F_{H_{n_1}H_{n_2}}(Q^2) = \int_0^\infty dz\, V(Q,z)\phi_{n_1}(z)\phi_{n_2}(z)\,, \tag{33}$$

where

$$\phi_n(z) = \sqrt{\frac{2}{\Gamma(n-1)}}\,\kappa^{n-1}\, z^{n-3/2}\, e^{-\kappa^2 z^2/2} \tag{34}$$

is the bulk profile of the AdS field dual to a hadron with n constituents [2, 18]. Straightforward calculation gives

$$\begin{aligned} F_{H_{n_1}H_{n_2}}(Q^2) &= \frac{\Gamma(\frac{n_1+n_2}{2})\,\Gamma(\frac{n_1+n_2}{2}-1)}{\sqrt{\Gamma(n_1-1)\Gamma(n_2-1)}}\,\frac{\Gamma(a+1)}{\Gamma(a+1+\frac{n_1+n_2}{2}-1)} \\ &\sim \frac{1}{a^{(n_1+n_2)/2-1}}\,, \end{aligned} \tag{35}$$

where $a = Q^2/(4\kappa^2)$. As before, the power of z in the bulk profile uniquely fixes the Q^2 scaling.

The latter formula reproduces the correct scaling of form factors with the corresponding number of partons (here, n is the number of $q\bar{q}$ pairs):

$$F_{H_n} \sim \left(\frac{1}{Q^2}\right)^{n-1}\,, \tag{36}$$

and gives a prediction for the production of single and double tetraquarks. In particular, the scaling of the form factor corresponding to $\gamma^* \to Z_c^+ + \pi^-$ is

$$F_{Z_c^+\pi^-} \sim \frac{1}{Q^4} \sim \frac{1}{s^2}\,, \tag{37}$$

in case of tetraquark structure of Z_c state, and

$$F_{Z_c^+\pi^-} \sim \frac{1}{Q^2} \sim \frac{1}{s}\,, \tag{38}$$

in the case when Z_c^+ is a system of two tightly bound diquarks.

For $\gamma^* \to Z_c^+ + Z_c^-$,

$$F_{Z_c^+Z_c^-} \sim \frac{1}{Q^6} \sim \frac{1}{s^3}\,, \tag{39}$$

in case of a Z_c state with tetraquark structure, and

$$F_{Z_c^+Z_c^-} \sim \frac{1}{Q^2} \sim \frac{1}{s}\,, \tag{40}$$

in case when Z_c^+ is a system of two tightly bound diquarks. These results are consistent with the scaling laws discussed in Ref. [17] [see Eqs. (5) and (6) in that reference]. Our results also agree with the counting rule for exclusive tetraquark-plus-meson production discussed in Ref. [19].

IV. APPLICATIONS TO STANDARD MODEL PROCESSES

We can also extend our analysis of exclusive processes to standard-model electroweak reactions such as $e^+e^- \to W^+W^- \to \rho^+W^-$ and $e^+e^- \to W^+W^- \to \rho^+\rho^-$. An example involving ν_e exchange is illustrated in Fig. 6. The virtual W^+ couples to the charged vector meson via coupling to its $\bar{u}d$ valence quarks.

The cross section for W-pair production in e^+e^- annihilation with one-loop corrections, along with earlier references, is given in Ref. [20]. Neutrino exchange gives the dominant contribution for $s \gg -t \gg M_W^2$:

$$\frac{d\sigma}{dt}(e^+e^- \to W^+W^-) \simeq \frac{\alpha_{\rm em}^2}{4\sin^4\theta_W}\,\frac{|t|}{4sM_W^4}\,. \tag{41}$$

In the case $s \gg M_W^2 \gg -t$, we obtain:

$$\frac{d\sigma}{dt}(e^+e^- \to W^+W^-) \simeq \frac{\alpha_{\rm em}^2}{4\sin^4\theta_W}\,\frac{1}{s|t|}\,. \tag{42}$$

The energy dependence for $s \gg M_W^2 \gg -t$ at fixed t is consistent with expectations for spin-$\frac{1}{2}$ exchange.

As is the case for $e^+e^- \to \gamma\gamma^* \to \gamma V^0$ reactions, the effect of hadron compositeness is to modify the analytic dependence in t of the exclusive cross section by a monopole form factor at $s \gg -t \gg M_W^2$:

$$\frac{d\sigma}{dt}(e^+e^- \to W^-W^{*+} \to W^-V^+) \simeq \frac{\pi\alpha_{\rm em}^3|V_{ud}|^2}{4\sin^6\theta_W}\,\frac{G_V^2(-t)\,M_\rho^2|t|}{4sM_W^6} \sim \alpha_{\rm em}^3|V_{ud}|^2\,\frac{\kappa^2M_\rho^2}{sM_W^6}\,. \tag{43}$$

In the case $s \gg M_W^2 \gg -t$, we find:

$$\frac{d\sigma}{dt}(e^+e^- \to W^-W^{*+} \to W^-V^+) \simeq \frac{\pi\alpha_{\rm em}^3|V_{ud}|^2}{4\sin^6\theta_W}\,\frac{G_V^2(-t)\,M_\rho^2}{2sM_W^4} \sim \alpha_{\rm em}^3|V_{ud}|^2\,\frac{\kappa^2M_\rho^2}{s|t|M_W^4}\,. \tag{44}$$

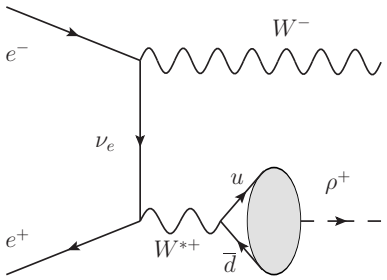

FIG. 6: Diagram contributing to the exclusive standard model hadronic amplitude $e^+e^- \to W^{*+}W^- \to \rho^+W^-$ via t-channel neutrino exchange.

Remarkably, the differential cross section is independent of t when $s \gg -t \gg M_W^2$, and the integrated cross sections for these exclusive hadronic reactions satisfy the leading-twist asymptotic scaling of the form $sR_{e^+e^-}(s) \sim$ const, despite the compositeness of the vector mesons.

Similar results also hold for neutral vector meson reactions such as $e^+e^- \to Z^{*0}Z^0 \to V^0Z^0$ and $e^+e^- \to Z^{*0}Z^{*0} \to V^0V^0$. These processes can all be studied at the proposed high-energy International Linear Collider [21].

V. CONCLUSIONS

We have seen that constituent counting rules can be used to develop interesting predictions for a variety of production processes in the forward and backward directions for exclusive $C = +$ annihilation processes involving fermion exchange, such as $e^+e^- \to \gamma V^0$ and $e^+e^- \to V^0V^0$. In such cases, keeping separate track of powers of $1/s$ and $1/|t|$ leads to interesting predictions, depending upon the states produced. The power-law falloff in the Mandelstam variables due to hadron compositeness can be determined both through the use explicit AdS/QCD soft-wall models and through consideration of the underlying quark amplitudes.

Processes in which a meson is created by a single photon introduce a transition form factor that must scale as $1/|t|^{1/2}$ for $-t \gg \Lambda_{\rm QCD}^2$, so that, for example, the differential cross section for $e^+e^- \to \gamma\gamma$ in the forward direction scales as $1/(s|t|)$ when $s \gg -t \gg \Lambda_{\rm QCD}$, but the exclusive cross section for $e^+e^- \to \gamma\rho^0$ in the forward direction scales as $1/(st^2)$ in the same kinematical limit. Similarly interesting results hold for high-energy electroweak processes such as forward-angle production $e^+e^- \to \rho^+W^-$, which must await the construction of the International Linear Collider.

The consequences of the constituent counting rules have also been verified here using AdS/QCD soft-wall models for the form factors of multiquark exotic hadrons. A core message of this paper is precisely the same as that which informs much of the work using constituent counting rules: In order to force a number of elementary constituents created at high energies and at large relative angles into hadrons in which they have small relative momenta, a number of hard constituents must be exchanged between them in order to produce bound hadronic states. This effect will only become more pronounced as experiments reach ever higher energies.

Acknowledgments

We thank Feng-Kun Guo for an exchange that inspired us to undertake this work. We also thank Michael Peskin for helpful conversations. This research was supported by the U.S. Department of Energy, contract DE–AC02–76SF00515 (SJB), by the U.S. National Science Foundation under Grant No. PHY-1403891 (RFL), by the German Bundesministerium für Bildung und Forschung (BMBF) under Project 05P2015 - ALICE at High Rate (BMBF-FSP 202): "Jet and fragmentation processes at ALICE and the parton structure of nuclei and structure of heavy hadrons", by Tomsk State University Competitiveness Improvement Program, and the Russian Federation program "Nauka" (Contract No. 0.1526.2015, 3854) (VEL). SLAC-PUB-16809.

.

[1] M. Davier, M.E. Peskin, and A. Snyder, hep-ph/0606155.
[2] S.J. Brodsky and G.F. de Téramond, Phys. Rev. D **77**, 056007 (2008) [arXiv:0707.3859 [hep-ph]].
[3] T. Branz, T. Gutsche, V.E. Lyubovitskij, I. Schmidt, A. Vega, Phys. Rev. D **82**, 074022 (2010) [arXiv:1008.0268 [hep-ph]].
[4] J.J. Sakurai, Ann. Phys. **11**, 1 (1960).
[5] G. Ecker, J. Gasser, A. Pich, and E. de Rafael, Nucl. Phys. B **321**, 311 (1989).
[6] G. Ecker, J. Gasser, H. Leutwyler, A. Pich, and E. de Rafael, Phys. Lett. B **223**, 425 (1989).
[7] S.J. Brodsky and G.R. Farrar, Phys. Rev. Lett. **31**, 1153 (1973).
[8] V.A. Matveev, R.M. Muradian, and A.N. Tavkhelidze, Lett. Nuovo Cim. **7**, 719 (1973).
[9] G.P. Lepage and S.J. Brodsky, Phys. Rev. D **22**, 2157 (1980).
[10] F.-K. Guo, U.-G. Meissner, and W. Wang, arXiv:1607.04020 [hep-ph].
[11] A. Karch, E. Katz, D.T. Son and M.A. Stephanov, Phys. Rev. D **74**, 015005 (2006) [hep-ph/0602229].
[12] S.J. Brodsky, G.F. de Téramond, and A. Deur, Phys. Rev. D **81**, 096010 (2010) [arXiv:1002.3948 [hep-ph]].
[13] A.P. Trawiński, S.D. Głazek, S.J. Brodsky, G.F. de Téramond, and H.G. Dosch, Phys. Rev. D **90**, 074017 (2014) [arXiv:1403.5651 [hep-ph]].
[14] T. Gutsche, V.E. Lyubovitskij, I. Schmidt, and A. Vega, Phys. Rev. D **90**, 096007 (2014) [arXiv:1410.3738 [hep-ph]].
[15] K.A. Olive *et al.* (Particle Data Group Collaboration), Chin. Phys. C **38**, 090001 (2014).
[16] S.J. Brodsky, F.-G. Cao, and G.F. de Téramond, Phys. Rev. D **84**, 075012 (2011) [arXiv:1105.3999 [hep-ph]].
[17] S.J. Brodsky and R.F. Lebed, Phys. Rev. D **91**, 114025 (2015) [arXiv:1505.00803 [hep-ph]].
[18] T. Gutsche, V.E. Lyubovitskij, I. Schmidt, and A. Vega, Phys. Rev. D **89**, 054033 (2014) [Phys. Rev. D **92**, 019902 (2015)] [arXiv:1306.0366 [hep-ph]].
[19] M.B. Voloshin, Phys. Rev. D **94**, 074042 (2016) [arXiv:1608.00238 [hep-ph]].
[20] R. Philippe, Phys. Rev. D **26**, 1588 (1982).
[21] N. van der Kolk [ILC Physics and Detector Study Group Collaboration], PoS DIS2016, 245 (2016) [arXiv:1607.00202 [hep-ex]].